Cell Transplantation, Vol. 26, pp. 1001–1016, 2017
Printed in the USA.

0963-6897/17 $90.00 + .00
DOI: https://doi.org/10.3727/096368916X694391
E-ISSN 1555-3892
www.cognizantcommunication.com

Human Dental Pulp Stem Cells Are More Effective Than Human Bone Marrow-Derived Mesenchymal Stem Cells in Cerebral Ischemic Injury

Miyeoun Song,*† Jae-Hyung Lee,†‡ Jinhyun Bae,§ Youngmin Bu,§ and Eun-Cheol Kim*

*Department of Oral and Maxillofacial Pathology, Research Center for Tooth and Periodontal Regeneration (MRC), School of Dentistry, Kyung Hee University, Seoul, Republic of Korea
†Department of Life and Nanopharmaceutical Sciences, Kyung Hee University, Seoul, Republic of Korea
‡Department of Maxillofacial Biomedical Engineering, School of Dentistry, Kyung Hee University, Seoul, Republic of Korea
§Department of Herbal Pharmacology, College of Oriental Medicine, Kyung Hee University, Seoul, Republic of Korea

We compared the therapeutic effects and mechanism of transplanted human dental pulp stem cells (hDPSCs) and human bone marrow-derived mesenchymal stem cells (hBM-MSCs) in a rat stroke model and an in vitro model of ischemia. Rats were intravenously injected with hDPSCs or hBM-MSCs 24 h after middle cerebral artery occlusion (MCAo), and both groups showed improved functional recovery and reduced infarct volume versus control rats, but the hDPSC group showed greater reduction in infarct volume than the hBM-MSC group. The positive area for the endothelial cell marker was greater in the lesion boundary areas in the hDPSC group than in the hBM-MSC group. Administration of hDPSCs to rats with stroke significantly decreased reactive gliosis, as evidenced by the attenuation of MCAo-induced $GFAP^+/nestin^+$ and $GFAP^+/Musashi\text{-}1^+$ cells, compared with hBM-MSCs. In vivo findings were confirmed by in vitro data illustrating that hDPSCs showed superior neuroprotective, migratory, and in vitro angiogenic effects in oxygen–glucose deprivation (OGD)-injured human astrocytes (hAs) versus hBM-MSCs. Comprehensive comparative bioinformatics analyses from hDPSC- and hBM-MSC-treated in vitro OGD-injured hAs were examined by RNA sequencing technology. In gene ontology and KEGG pathway analyses, significant pathways in the hDPSC-treated group were the MAPK and TGF-β signaling pathways. Thus, hDPSCs may be a better cell therapy source for ischemic stroke than hBM-MSCs.

Key words: Human dental pulp stem cells (hDPSCs); Stroke; Cell therapy; Oxygen–glucose deprivation (OGD); Intravenous injection

INTRODUCTION

Stroke remains a leading cause of death and disability worldwide, with only 3% of the ischemic stroke patient population benefiting from the thrombolytic drug tissue plasminogen activator (TPA)[1]. Once cell damage from stroke is established, little can be done to restore prestroke conditions. Recent animal studies and preclinical trials have investigated human-derived cells of different origins, such as human mesenchymal stem cells (hMSCs), human bone marrow-derived MSCs (hBM-MSCs), human umbilical cord blood cells (hUCBCs), human adipose tissue-derived MSCs (hADSCs), and human neural stem cells (hNSCs), as potential sources for cell therapy for the treatment of stroke[2–4]. However, the methods used to acquire these stem cells are invasive and painful for the donor.

Human dental pulp stem cells (hDPSCs) are neural crest-derived stem cells residing within the perivascular niche of the dental pulp[5]. hDPSCs appear to be an excellent source of stem cells because they can be obtained without adverse health effects and can be obtained non-invasively from extracted teeth discarded as medical waste, avoiding many ethical issues[6]. hDPSCs show higher self-renewal ability, immunomodulatory capacity, and proliferation in vitro than hBM-MSCs, and they can differentiate into muscle, cartilage, bone, and other cell types in vitro and in vivo[5,7]. Moreover, DPSCs have been reported to have the potential for use in cell-based therapy for systemic diseases, such as neurological diseases and cardiac disease, and to ameliorate ischemic disease[8–10].

In vitro studies have shown that hDPSCs can differentiate toward functionally active neurons under

Received December 3, 2015; final acceptance March 29, 2017. Online prepub date: January 20, 2017.
Address correspondence to Eun-Cheol Kim, D.D.S., Ph.D., Professor, Department of Oral and Maxillofacial Pathology, Research Center for Tooth and Periodontal Regeneration (MRC), School of Dentistry, Kyung Hee University, 26 Kyungheedae-ro, Dongdaemun-gu, Seoul 130-701, Republic of Korea. Tel: +82-2-961-0383; Fax: +82-2-960-2324; E-mail: eckim@khu.ac.kr

appropriate culture conditions[11–13]. Furthermore, in vivo studies have demonstrated that stem cells from porcine dental pulp promote a high degree of vascularization in hindlimb ischemia[14], and these cells, when transplanted into the rat brain, promoted migration and neurogenic differentiation and ameliorated ischemic brain injury after middle cerebral artery occlusion (MCAo)[8]. Moreover, intracerebral transplantation of hDPSCs enhanced post-stroke functional recovery in a rodent model[12]. However, intracerebral injection is an invasive procedure that involves infrequent but significant risks, including further strokes[15], whereas intravenous (IV) injection is clinically safe.

To our knowledge, no comparative study of the therapeutic potential of IV transplantation of hDPSCs and hBM-MSCs in a rat stroke model has been reported. The aim of this study was to investigate whether IV-administered hDPSCs migrate to the lesion boundary area, differentiate into neuronal cells, and improve functional recovery after stroke in MCAo-induced rats, compared with hBM-MSCs. Neuroprotective, migratory, and angiogenic abilities of hDPSCs and hBM-MSCs were evaluated in ischemic human astrocytes (hAs), an in vitro model of stroke. Furthermore, RNA sequencing (RNA-Seq) transcriptional profiling was used to gain insight into the molecular mechanism of the in vitro model.

MATERIALS AND METHODS

Primary Culture of hAs, hBM-MSCs, and hDPSCs

Human dental pulp tissues ($n=10$) were obtained from the third molars or premolars, extracted for orthodontic treatment, from patients (four males, six females, 14–22 years old) at the Department of Oral Surgery, Kyung Hee Dental Hospital (Seoul, Republic of Korea). Informed consent was obtained from each patient before the extractions. The ethics committee of Kyung Hee University (Seoul, Republic of Korea) approved the procedure and the experimental protocol. The study conformed to the 2013 WMA Declaration of Helsinki. hDPSCs were isolated and cultured as described previously[5]. Briefly, the pulp was immersed in a digestive solution [type I collagenase (3 mg/ml; Merck Millipore, Darmstadt, Germany) plus dispase (4 mg/ml; Gibco; Thermo Fisher Scientific, Karlsruhe, Germany) in phosphate-buffered saline (PBS; Invitrogen; Thermo Fisher Scientific) containing 100 U/ml penicillin and 100 mg/ml streptomycin (Gibco)] for 1 h at 37°C with agitation. After filtration, primary cells were cultured in Dulbecco's modified Eagle's medium (DMEM) containing 10% fetal bovine serum (FBS; Sigma-Aldrich, St. Louis, MO, USA) and antibiotics. $CD34^+/c\text{-}kit^+/STRO\text{-}1^+$ hDPSC population was sorted from the primary cultured dental pulp cells by a magnetic-activated cell sorting method as described previously[16,17]. hDPSCs were used at passages 3–5.

Primary hAs were purchased from Gibco BRL (Grand Island, NY, USA) and cultured in hA medium (Gibco) supplemented with DMEM, N-2, and 10% FBS at 37°C in 5% CO_2. hAs were grown on Geltrex-coated tissue culture vessels; overexposure to light was avoided. hAs were used at passages 7–9. Cultures were monitored regularly for the expression of the astrocyte marker glial fibrillary acidic protein (GFAP) using immunofluorescence staining.

Human MSCs from three different healthy donors (19–24 years, two males) were isolated from bone marrow aspirate obtained by Lonza (Lonza, Walkersville, MD, USA). hBM-MSCs were cultured in mesenchymal stem cell basal medium (MSCBM; Cambrex Bio Science, Verviers, Belgium), supplemented with mesenchymal cell growth supplement (Cambrex Bio Science), L-glutamine, (Gibco; Thermo Fisher Scientific), and antibiotics (penicillin/streptomycin; Gibco; Thermo Fisher Scientific), at 37°C in a 5% CO_2 atmosphere. In this study, hBM-MSCs were used prior to their fifth passage.

Animal MCAo Model and Cell Transplantation Procedure

All experimental procedures were approved by the Institutional Animal Care and Use Committee (IACUC) of Kyung Hee University (Seoul, Republic of Korea). Adult male Sprague–Dawley rats weighing 250–300 g (Orient Bio Inc., Seoul, Republic of Korea) were used. Transient focal cerebral ischemia was induced using intraluminal thread occlusion of the left middle cerebral artery (MCAo), as described previously[18]. Briefly, transient focal cerebral ischemia was induced by intraluminal thread occlusion of the MCA for 2 h followed by reperfusion. During brain ischemia, rectal temperature was maintained at 37 ± 0.5°C using a thermistor-controlled heated blanket. At 24 h after surgery, rats were assessed for forelimb flexion and contralateral circling to confirm the presence of ischemia. Originally, 12 rats were used simultaneously, but rats with a normal behavioral pattern after surgery or those that were found dead were excluded. Thus, nine rats per group were evaluated.

Three experimental groups were used: MCAo+PBS injection [PBS-injected rats with the MCAo model (PI; $n=9$), MCAo+hDPSC injection (hDPSCs injected into MCAo model rats (hDI; $n=9$), and MCAo+hBM-MSC injection (hBM-MSC-injected MCAo model rats (hMI; $n=9$)]. hDPSCs or hBM-MSCs (4×10^6 cells in 500 µl of PBS) were administered via tail vein injection at 24 h after MCAo. hDPSCs and hBM-MSCs were harvested from three donors. All animals were randomly assigned to primary cultured hDPSCs or hBM-MSCs.

Experimental groups (PI, hDI, and hMI) were tested three different times.

Behavioral Tests

The modified neurological severity score (mNSS) test was performed at 1, 7, 14, 21, and 28 days ($n=9$ for each group) after MCAo by two individuals blinded to the experimental groups. The mNSS test is a composite of motor, sensory, reflex, and balance tests[2,19]. Neurological function was graded on a scale of 0 to 18 (normal score=0, maximal deficit score=18).

Histological Assessment

Rats were sacrificed 28 days after MCAo. Briefly, animals were anesthetized and perfused through the heart with 100 ml of cold saline (Sigma-Aldrich), followed by 100 ml of 4% paraformaldehyde (PFA) in 0.1 M phosphate buffer (Sigma-Aldrich). Brains were postfixed in the same fixative for 24 h, followed by immersion in 30% sucrose (Sigma-Aldrich) for 24 h, and sectioning on a cryostat (Leica CM 1900; Leica, Milton Keynes, UK) at 30 μm. Other organs, such as the liver and kidney, were also collected for histological examination.

To measure infarct volume, five sections of brains at 2-mm intervals at 28 days after MCAo ($n=5$ per group) were collected for Nissl staining. Analysis was performed using ImageJ software [National Institutes of Health (NIH), Bethesda, MD, USA]. The total volumes of both the contralateral and ipsilateral hemispheres and the volumes of the striatum and cortex in both hemispheres were measured; the infarct (unstained) area was calculated as mm^3.

Single and Double Immunohistochemical Assessments

Briefly, sections were incubated with primary antibodies, such as anti-human nuclear matrix antigen (hNuA; mouse; 1:20; EMD Millipore, Temecula, CA, USA), neuronal nuclear antigen (NeuN; rabbit; 1:100; EMD Millipore), GFAP (1:1,000; rabbit; EMD Millipore), von Willebrand factor (vWF; rabbit; 1:200; Sigma-Aldrich), nestin (rabbit; 1:200; EMD Millipore), and Musashi-1 (mouse; 1:40; R&D Systems, Minneapolis, MN, USA). Alexa fluor-conjugated secondary antibodies (1:200; Molecular Probes, Eugene, OR, USA) were used for double-labeled immunoreactivity identification. Slides were counterstained with 4′,6-diamidino-2-phenylindole dihydrochloride (DAPI) and coverslipped. The antibodies were then detected at the appropriate wavelength using confocal microscopy (Cell Voyager CV1000; Yokogawa Electric Corporation, Tokyo, Japan). For negative controls, the primary antibody was omitted, and sections were incubated in normal serum alone. Analysis of the vWF^+-stained area, GFAP/Musashi-1^+-stained area, and GFAP/$nestin^+$ cells was based on the evaluation of at least five randomly selected fields of view (objective magnification: 200×) from an average of five slides per experimental group using the ImageJ software (NIH). To quantify graft survival, $hNuA^+$ cells in the same focal plane were counted for at least five randomly selected fields of view (objective magnification: 200×) from an average of five slides per experimental group.

Coculture of hAs With hDPSCs or hBM-MSCs

Astrocytes (4×10^4/well) were cultured in 24-well plates. hDPSCs or hBM-MSCs (10^4 cells) were cocultured in the upper chamber of the Transwell cell inserts [0.4-μm pore size, transparent polyester (PET) membrane; BD Falcon, Franklin Lakes, NJ, USA] of the same plates (a 1:4 hDPSC/hBM-MSC-to-hAs ratio).

Oxygen–Glucose Deprivation (OGD) and Reoxygenation

The OGD insult followed by reoxygenation is an established model of ischemia in vitro, as described previously[19,20]. To induce OGD, the culture medium was replaced with glucose- and serum-free DMEM and deoxygenated using an anaerobic chamber (Bionex; Vision Scientific, Gyeonggi-do, Republic of Korea) with a 1% O_2, 94% N_2, and 5% CO_2 atmosphere for 2 h. hDPSCs and hBM-MSCs were incubated with astrocytes for an additional 2 h under reoxygenation conditions. The control culture was maintained in complete medium and put in the incubator under normal conditions.

Assessment of Cell Viability

Cell viability was assessed with the 3-[4,5-dimethylthialzol-2-yl]-2,5-diphenyltetrazolium bromide (MTT) assay. MTT (0.5 mg/ml) was added to stimulated cells for 3 h. After removal of medium and addition of dimethyl sulfoxide (DMSO), absorbance at 570 nm was measured using a microplate reader (Bio-Rad, Mississauga, ON, Canada).

Migration of hDPSCs or hBM-MSCs to Ischemic hAs

Astrocytes (4×10^4/well) were cultured in 24-well plates and then were incubated in the OGD state for 2 h. Then 5 mM calcein acetoxymethyl ester (calcein-AM; BD Falcon)-labeled hDPSCs or hBM-MSCs (10^4 cells) were cocultured in the upper chamber of Transwell cell inserts (3.0-μm pore size, transparent PET membrane; BD Falcon) of the same plates (a 1:4 hDPSCs/hBM-MSCs-to-hAs ratio) for 24 h. At the end of the coculture, the upper insert was removed, and then the cells on the bottom layer were fixed with 4% PFA. Cells were stained with DAPI, and migrated calcein-AM^+ cells were investigated by confocal laser microscopy (Cell Voyager CV1000).

In Vitro Angiogenesis Assay

Angiogenesis was determined using an in vitro angiogenesis assay kit (EMD Millipore) according to the manufacturer's protocol. hDPSCs and hBM-MSCs (4×10^5 cells) were cultured in serum-free endothelial cell medium (ECM; ScienCell Research Laboratories, Carlsbad, CA, USA). Conditioned medium (CM) was made by seeding hDPSCs or hBM-MSCs at a density of 20,000 cells/cm^2 in 25-cm^2 cell culture flasks. Cells were allowed to adhere overnight, washed twice with PBS, and incubated with 5 ml of standard culture medium containing 0.1 % FBS. Following 48 h of incubation, the CM was harvested and stored at −80°C.

Human umbilical vein endothelial cells (HUVECs; 1×10^4 cells/well) were seeded on ECM gel and were cultured with the CM described above at 37°C under a 5% CO_2 atmosphere for 16 h. Then five random fields of each well were analyzed for tube formation under an inverted light microscope (Olympus, Tokyo, Japan) at 40× magnification. The length and number of tubes per field were measured using the NIH ImageJ software (ver. 1.29; http://rsbweb.nih.gov/ij/).

Statistical Analyses

Statistical analyses were conducted using GraphPad Prism (ver. 6 for Windows; GraphPad Software, La Jolla, CA, USA). Differences between the two groups in terms of continuous variables were analyzed using Student's *t*-test, and for multiple comparisons, one-way analysis of variance (ANOVA) was used with the Bonferroni correction. Values of $p<0.05$ were considered to indicate statistical significance.

RNA Extraction and Sequencing

Total RNAs from ischemic damaged hAs with or without treatment with hDPSCs and hBM-MSCs were prepared. The integrity of extracted total RNA was analyzed with a BioAnalyzer (Agilent 2100 Bioanalyzer; Agilent Technologies, Santa Clara, CA, USA), and the standard Illumina protocol was used to prepare libraries for RNA-Seq. Using gel electrophoresis, around 300-bp fragments were isolated and amplified by polymerase chain reaction (PCR) and sequenced on an Illumina HiSeq 2000 in the paired-end sequencing mode (2× 101-bp reads).

RNA Sequencing Differential Gene Expression Analysis

Raw sequencing reads were preprocessed to remove sequencing adapters, and then reads were aligned to the human genome sequence (hg19) using Genomic Short-read Nucleotide Alignment Program (GSNAP)[21]. Only uniquely and properly mapped read pairs were used for further analysis. To identify differentially expressed genes, DESeq (http://www-huber.embl.de/users/anders/DESeq)[22] was used, and differentially expressed genes were defined as those with changes of at least 1.5-fold between a pair of samples at a false discovery rate (FDR) of 10%. Analysis of protein functional class for the upregulated genes in damaged hAs treated with hDPSCs or hBM-MSCs was performed using the Protein ANalysis THrough Evolutionary Relationships (PANTHER) tools (http://www.pantherdb.org/)[23].

Gene Ontology (GO) Term and Kyoto Encyclopedia of Genes and Genomes (KEGG) Term Pathway Enrichment Tests

GO term and KEGG pathway enrichment analyses were conducted similarly to that of a previous report[24]. Briefly, to test the GO term and KEGG pathway enrichment in a particular upregulated gene set, the fraction of genes in the test set (F_{test}) associated with each GO category was calculated. Then we created a random control gene set that had the same number of genes as the test set. In this process, a random control gene was picked by matching the length of the test gene. The fraction of genes in this randomly chosen control set ($F_{control}$) associated with the current GO category was calculated. This random sampling process was repeated 100,000 times to calculate an empirical *p* value. A *p* value cutoff (1/total number of GO terms considered) was applied to choose significantly enriched GO terms or KEGG pathways.

Computational Methods

The resulting *p* values from DESeq were corrected via the Benjamini and Hochberg method[68], as implemented in "R." For GO analysis, empirical *p* values were estimated based on 100,000 randomized simulations, and the Bonferroni cutoff was used to determine significant *p* values. To conduct hierarchal clustering and generate heatmaps for the mitogen-activated protein kinase (MAPK) signaling pathway and transforming growth factor-β (TGF-β) signaling genes, the MeV (ver. 4.8.1) package (http://www.tm4.org/mev.html) was used.

RESULTS

hDPSCs Promoted Functional Recovery and Reduced Infarct Volume

To determine whether the transplanted hDPSCs or hBM-MSCs could improve neurological function, mNSS was used. Neurological severity scores on day 1 did not differ significantly among the three groups. mNSS scores in the hDI and hMI groups on days 7, 14, 21, and 28 were lower than those in the control group ($p<0.05$), although there was no significant difference between the hDI and hMI groups (Fig. 1A).

The volume of the ischemia–reperfusion infarct was calculated in the Nissl-stained coronal sections of the rat brains. The MCAo resulted in cortical infarction and typically included most of the parietal sensorimotor cortex

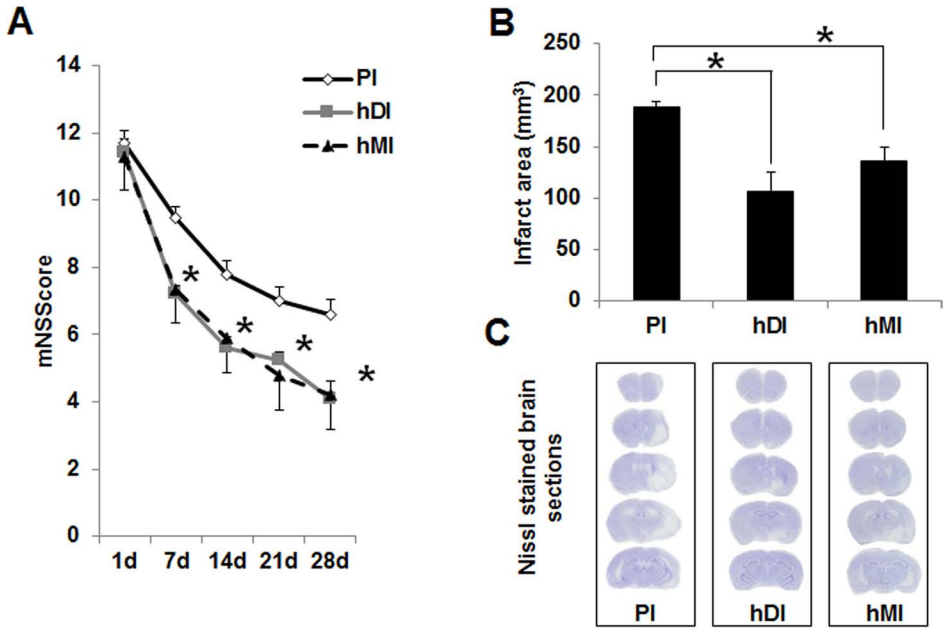

Figure 1. Effects of intravenous (IV) transplantation of human dental pulp stem cells (hDPSCs) and human bone marrow-derived mesenchymal stem cells (hBM-MSCs) on neurological function and infarct volume after middle cerebral artery occlusion (MCAo). (A) Functional recovery was assessed by a modified neurologic severity score (mNSS) test at days 7, 14, 21, and 28. PI, ischemia with PBS injection ($n=9$); hDI, ischemia with hDPSC injection ($n=9$); hMI, ischemia with hBM-MSC injection ($n=9$). (B) Infarct size of rat brains at 28 days after MCAo. Infarct volume measurements were performed on Nissl-stained coronal sections. (C) Nissl-stained brain sections of the PI, hDI, and hMI groups, respectively. Data are expressed as mean ± standard deviation (SD). *$p<0.05$ compared to the control group (Student's *t*-test).

(Fig. 1C). hDPSC and hBM-MSC transplantation significantly reduced the infarct volume, compared with the PBS group (hDI: 106.2±18.5 mm^3, hMI: 136.1±13.8 mm^3, PI: 187.9±6.1 mm^3; $p<0.05$). hDI (44% reduction) also showed a significantly decreased infarct volume versus hMI (28% reduction) (Fig. 1B).

IV-Administered hDPSCs Were Not Found in Systemic Organs

To detect any adverse reaction due to the hDPSCs, systemic organs such as the liver and kidney were examined in each hDPSC-transplanted animal. Immunohistochemical analysis for human nuclei antibody (hNuA), a specific marker for human cellular nuclei, was performed to assess the migration of injected hDPSCs in systemic organs. No $hNuA^+$ cells were found in systemic organs—including liver and kidney—in hDI animals. In contrast, a few human nuclei-positive cells were found in the liver and kidney in the hMI group.

IV-Administered hDPSCs Migrated to the Lesion Boundary Area in the Ischemic Rat Brain and Differentiated Into Astrocytes and Neurons

To determine whether injected hDPSCs or hBM-MSCs migrated and differentiated into neurons and astrocytes in the brains of the stem cell-transplanted rats, double-staining immunohistochemistry was performed in the brain regions of the ischemic hemisphere: ischemic core (Fig. 2A) and boundary zone (Fig. 2B). hDPSCs and hBM-MSCs, identified by neuronal marker hNuA immunoreactivity, survived and were distributed in lesion boundary areas in the damaged brains of recipient rats (Fig. 2B). As shown in Figure 2, some $hNuA^+$ cells (green for $hNuA^+$, blue for cell nucleus identification) colocalized with antibodies for NeuN and GFAP (red for neuron- and astrocyte-specific markers, respectively) in the brains of hDI- and hMI-injected rats.

To determine the relative efficacy of hDPSC and hBM-MSC transplantation in the ischemic lesion, the human NeuN- and GFAP-double-positive cells or $hNuA^+$ were counted in the brain tissue from total injected cells (4×10^6). As shown Figure 2C, quantitative analysis demonstrated that the number of $hNuA^+$ cells in the hDI group was significantly higher than that of the hMI group ($p<0.05$) (Fig. 2C).

IV-Administered hDPSCs Promoted Angiogenesis Significantly Versus the hBM-MSC-Injected Group in Ischemic Rat Brain and Inhibited Significantly Astrogliosis

Angiogenesis was identified by an endothelial marker: the vWF^+-stained area (mm^2) in the brains of rats.

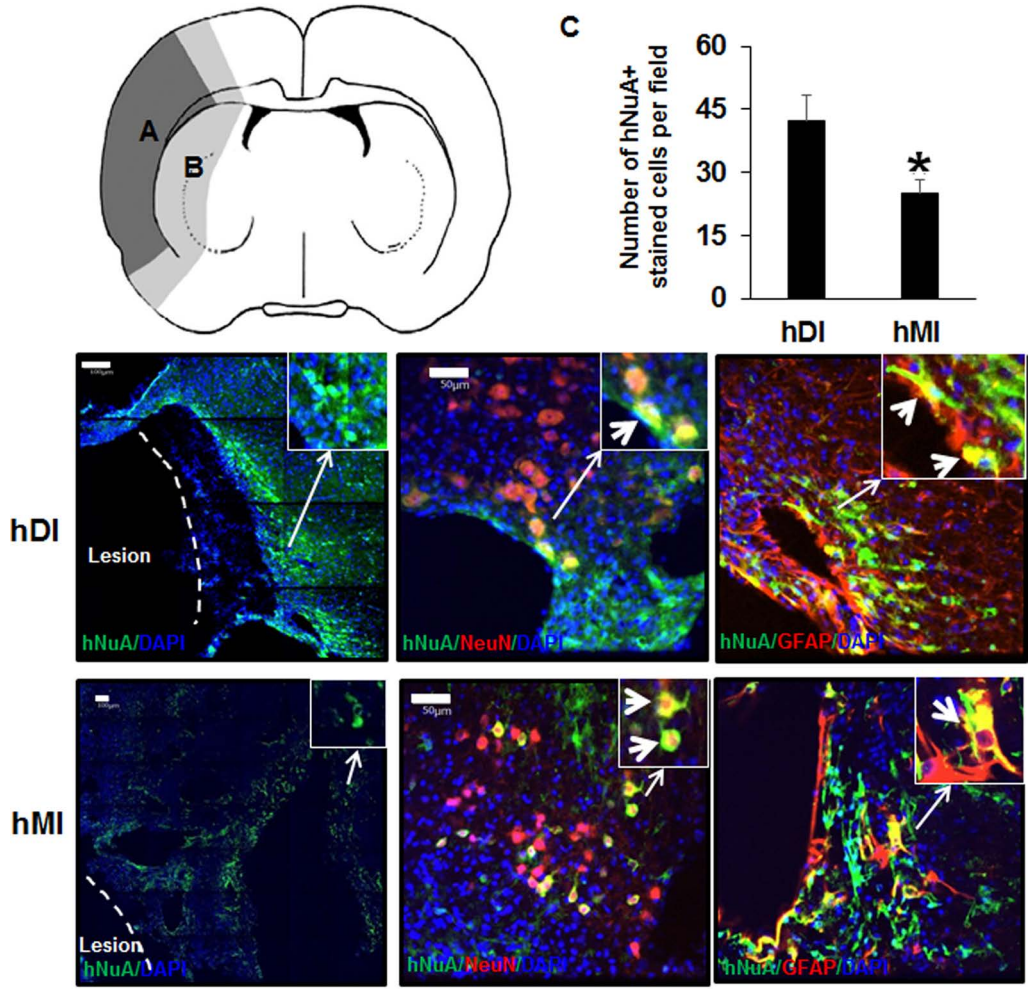

Figure 2. Immunohistochemical staining of rat brains to evaluate targeting migration and neurogenic differentiation of injected hDPSCs (hDI) or hBM-MSCs (hMI) 28 days after MCAo. Schematic diagram depicting the regions of transplanted cells. hDPSCs and hBM-MSCs were investigated in the brain regions of the ischemic hemisphere: (A) ischemic core indicated by dark gray; (B) boundary zone indicated by bright gray. Representative image of double staining of nucleus [4′,6-diamidino-2-phenylindole (DAPI), blue], human nucleus (hNuA, green), astrocytes [glial fibrillary acidic protein (GFAP), red], and neurons (NeuN, red). The right upper windows of images show high-magnification images of the arrow area. Thick arrows in the right upper windows indicate $hNuA^+/NeuN^+$ and $hNuA^+/GFAP^+$ cells. Scale bars: 100 μm (hNuA/DAPI-stained section images), 50 μm (hNuA/GFAP or hNuA/NeuN-stained section images). These images are representative of three independent experiments. (C) Quantification of human stem cells by human antibody immmunoreactivity in the rat brain. Data are expressed as mean ± SD. *$p < 0.05$ compared to the control group (Student's *t*-test).

Quantitative analysis demonstrated that the area of vWF staining in the hDI and hMI groups was higher than that in the PI group ($p < 0.05$). Moreover, the area of vWF staining in the hDI group was significantly higher than that in the hMI injection group ($p < 0.05$) (Fig. 3).

Because transplantation of hDPSCs and hBM-MSCs enhanced neurogenesis in the ischemic cortex of rats (Fig. 2), we next examined immunostaining for GFAP and nestin, which are induced in reactive astrocytes following brain injury (Fig. 3). Double-staining immunohistochemistry of brain sections revealed that $GFAP^+$ and $nestin^+$ cells were present in the ischemic boundary areas of MCAo rats at 28 days. Semiquantitative analysis showed that the hDI and hMI significantly decreased MCAo-induced $GFAP^+/nestin^+$ cells, compared with PI ($p < 0.05$) (Fig. 3). To further explore the effects of hDI and hMI on astrogliosis, we assessed the double fluorescence staining of GFAP and Musashi-1, a marker for reactive astrocytes (Fig. 4). hDI and hMI significantly suppressed the $GFAP^+/Musashi\text{-}1^+$-stained area, compared with PI ($p < 0.05$). However, the effects of hDI were similar to those observed in the hMI-treated groups.

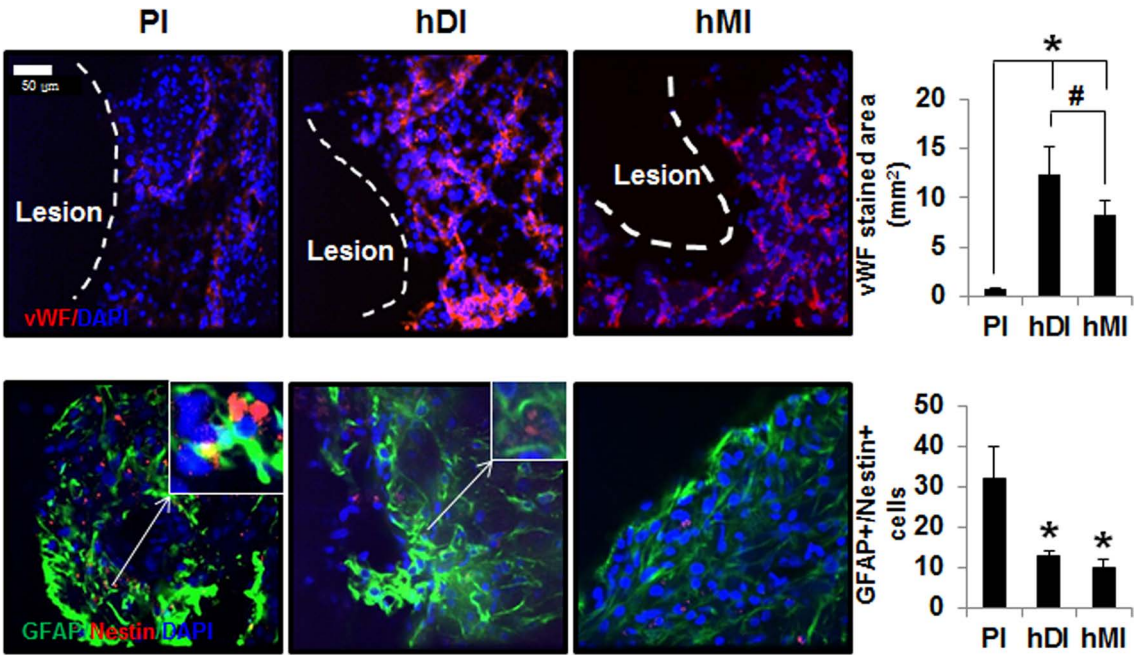

Figure 3. Immunohistochemical staining of rat brains to evaluate angiogenesis and astrogliosis of hDI or hMI 28 days after MCAo. Representative image of double staining of nucleus (DAPI, blue), von Willebrand factor (vWF, red), GFAP (green), and nestin (red). Scale bar: 50 μm. Positive cells and areas in the brain from MCAo rats were analyzed using an image analyzer. The right upper windows of images show high-magnification images of the arrow area. The thick arrow in right upper windows indicates $GFAP^+$/$nestin^+$ cells. vWF^+ (A) and double-labeled (GFAP and nestin; B) cells were counted in three to five coronal sections per animal ($n=5$). Data are expressed as mean ± SD. *$p<0.05$ compared to the control group (Student's *t*-test); #$p<0.05$ compared to each group (Student's *t*-test).

hDPSCs Reduced Cell Death in OGD-Induced hAs, Migrated to Ischemic hAs, and Promoted In Vitro Angiogenesis

To further examine the effects of hDI or hMI in an in vitro model of stroke, OGD and reperfusion-exposed hAs were posttreated with hDI or hMI. As shown in Figure 5A, exposure to OGD for 2 h and reperfusion for 2 h induced a significant decrease in the cell viability of hAs. However, posttreatment with hDI or hMI protected hAs against OGD-induced injury. Consistent with the in vivo findings, the neuroprotective effects of hDI were significantly superior to those of hMI ($p<0.05$). The migration of calcein-AM-labeled hDI and hMI was evaluated in an in vitro Transwell culture system (Fig. 5C). hDI showed more cell migration than the hMI group (Fig. 5B).

To examine whether hDPSCs and hBM-MSCs induce angiogenesis, an in vitro capillary-like tube formation assay in a HUVEC model was performed. As shown in Figure 5D, CM from hDPSCs and hBM-MSCs increased capillary-like tube formation in HUVECs, compared with HUVECs incubated with control culture medium. The number and total length of tubular structures per well in CM from hDPSCs increased significantly in HUVECs relative to those treated with CM from hBM-MSCs ($p<0.05$) (Fig. 5E and F).

Genes Differentially Regulated by hDPSC- or hBM-MSC-Treated OGD-Damaged hAs

To understand the differential gene regulation, we compared the gene expression profiles between OGD-damaged hAs treated with hDPSCs and hBM-MSCs. In each comparison, more than 31,000 Ensembl genes (release 75) were used for the differential gene expression tests. When we applied a fold-change difference of 1.5 and an FDR of 10%, 196 and 121 genes were differentially expressed between treatment of OGD-injured hAs with hDPSCs and hBM-MSCs, respectively (Fig. 6A). Focusing on upregulated genes in the treated groups, many interesting protein classes were detected based on PANTHER protein class categories[23] (Fig. 6B). The fractions of "receptor," "hydrolase," and "signaling molecule" classes in the upregulated genes in the hDPSC group were larger than those in the hBM-MSC group. The fractions of structural proteins and transcription factors showed the opposite trend.

To investigate the functional significance of the upregulated genes, we performed functional enrichment

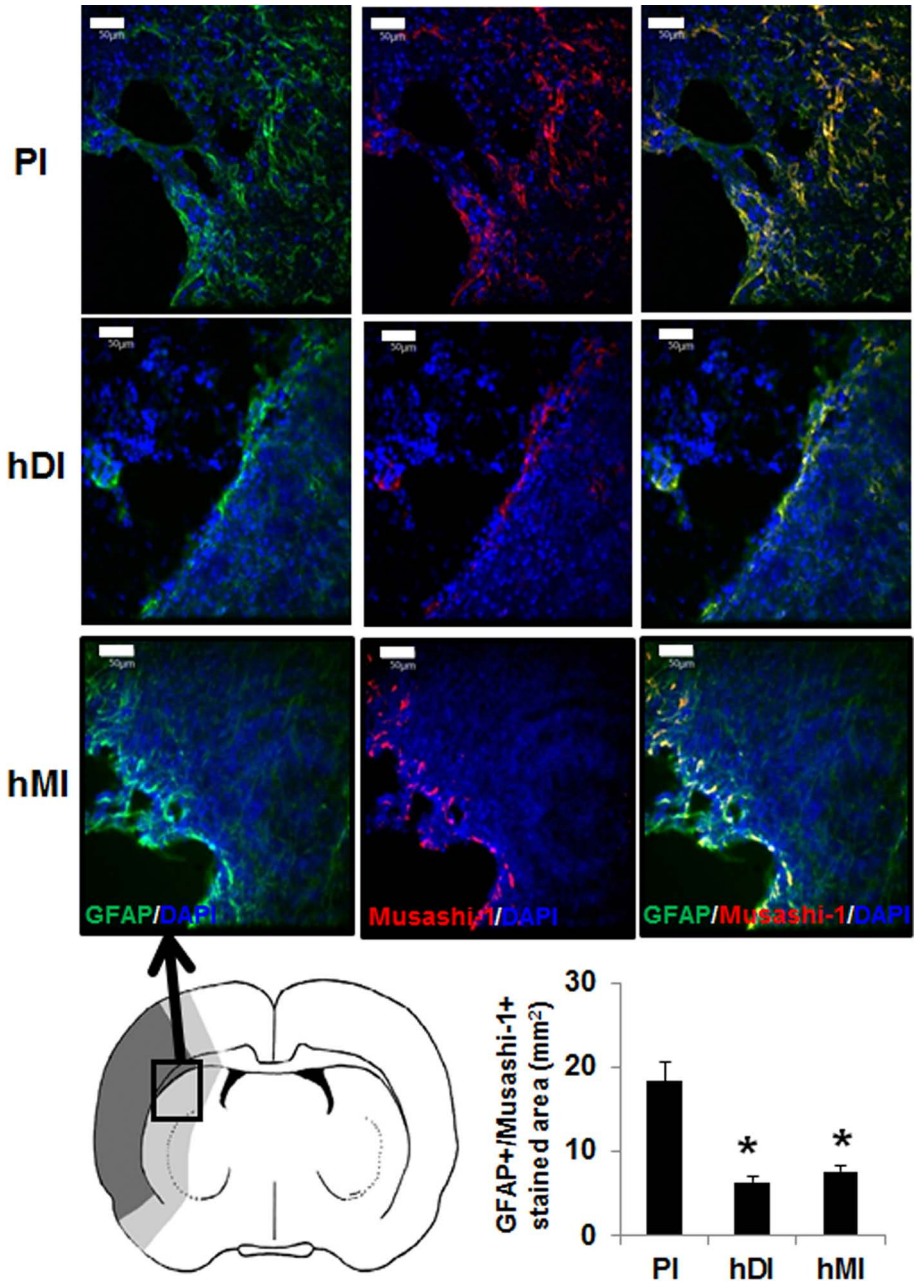

Figure 4. Immunohistochemical staining of rat brains to evaluate astrogliosis using GFAP/Musashi-1 staining of injected hDPSCs (hDI group) or hBM-MSCs (hMI group) 28 days after MCAo. Schematic diagram depicting the regions of transplanted cells sampled for quantitative analyses. Ischemic core is indicated by dark gray, and boundary zone is indicated by bright gray. Representative image of double staining of nucleus (DAPI, blue), GFAP (green), and Musashi-1 (red). Scale bars: 50 μm. Positive stained areas ($GFAP^+$/$Musashi\text{-}1^+$ cells) in the brain from MCAo rats were analyzed using an image analyzer. GFAP and Musashi-1 double-stained areas were measured in three to five coronal sections per animal ($n=5$). Data are expressed as mean ± SD. *$p<0.05$ compared to the control group (Student's *t*-test).

tests using GO terms and KEGG pathways. As shown in Figure 6C, many interesting GO terms or KEGG pathways in hDPSCs or hBM-MSCs were significantly enriched: (1) cellular processes, such as "positive regulation of cell proliferation," "negative regulation of apoptotic process," "positive regulation of cell migration," "positive regulation of angiogenesis," "positive regulation of cell differentiation," and "positive regulation of cell differentiation"; (2) signaling pathways, such as "ERK1 and ERK2 cascade," "Janus-activated kinase

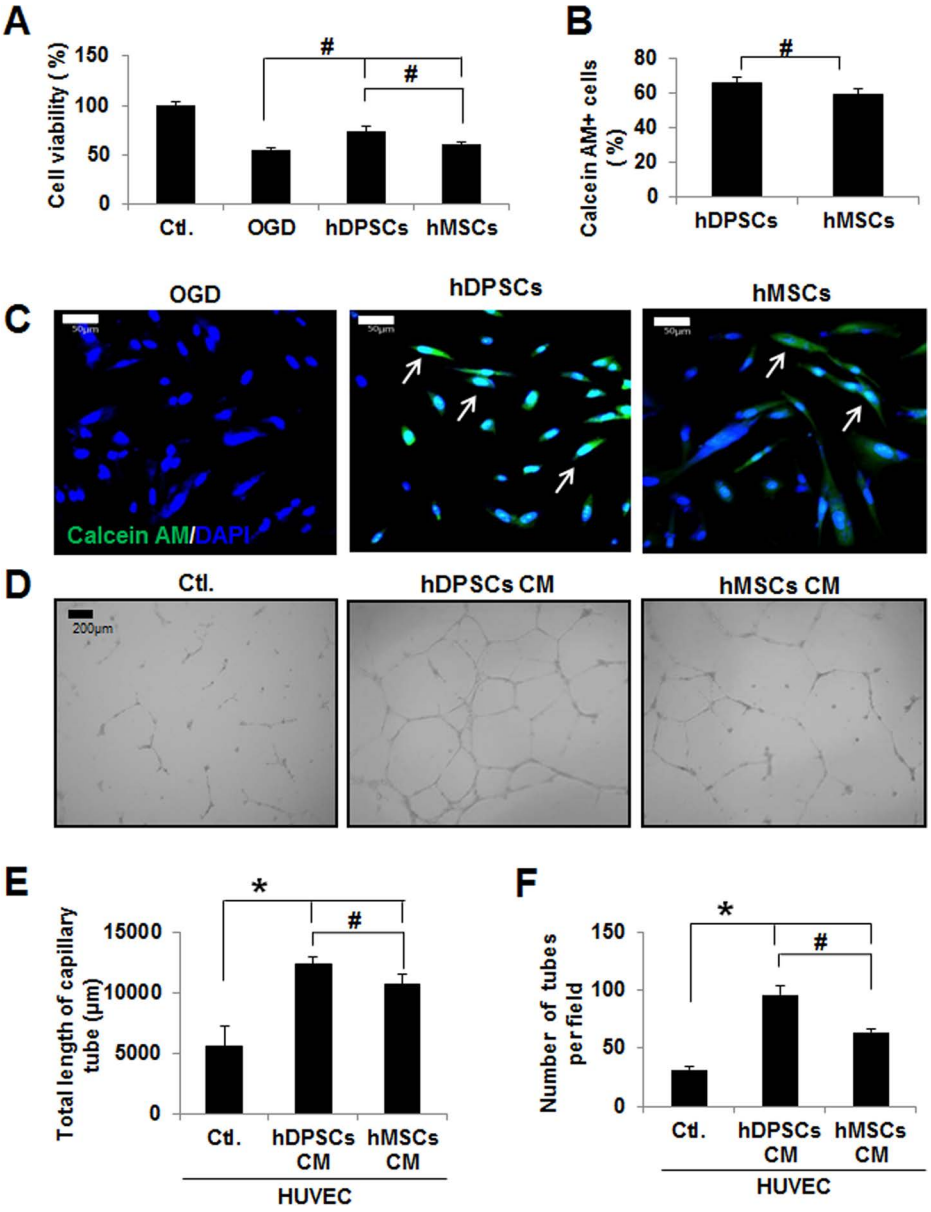

Figure 5. Effect of hDPSCs and hBM-MSCs on cell viability (A), migration (B, C), and angiogenesis (D, E) in oxygen–glucose deprivation (OGD)-injured human astrocytes (hAs). (A) hA cell viability was measured by 3-(4,5-dimethylthiazol-2-yl)-2,5-diphenyltetrazolium bromide (MTT) assay. Data are representative of three independent experiments. Ctl., control. (B) Graph showing that hDPSCs or hBM-MSCs migrated to ischemic hAs in the Transwell system. (C) Representative image of migration of hDPSCs or hBM-MSCs to ischemic hAs. Calcein acetoxymethyl ester (calcein AM)/DAPI double-positive cells indicate migrated hDPSCs or hBM-MSCs. (D) Representative capillary formation with conditioned medium (CM) obtained from hDPSC- and hBM-MSC-treated human umbilical vein endothelial cells (HUVECs). The graph shows the average total length of capillary tube (μm) (E) and number of tubes per field (F) in three independent experiments. Data are expressed as mean ± SD ($n = 5$). *$p < 0.05$ compared to the control group (Student's *t*-test); #$p < 0.05$ compared to each group (Student's *t*-test).

(JAK)-signal transducer and activator of transcription (STAT) signaling pathway," "mitogen-activated protein kinase (MAPK) activity," and "transforming growth factor-β (TGF-β) signaling pathway"; and (3) known OGD phenomena, such as "angiogenesis" and "response to hypoxia."

hDPSC and hBM-MSC Treatment in OGD-Damaged hAs Affected Gene Regulation in the MAPK and TGF-β Signaling Pathways

To systematically search the transcriptome data for the subset of genes with >1.5-fold differential expression in hDPSC- and hBM-MSC-treated hAs, the variance

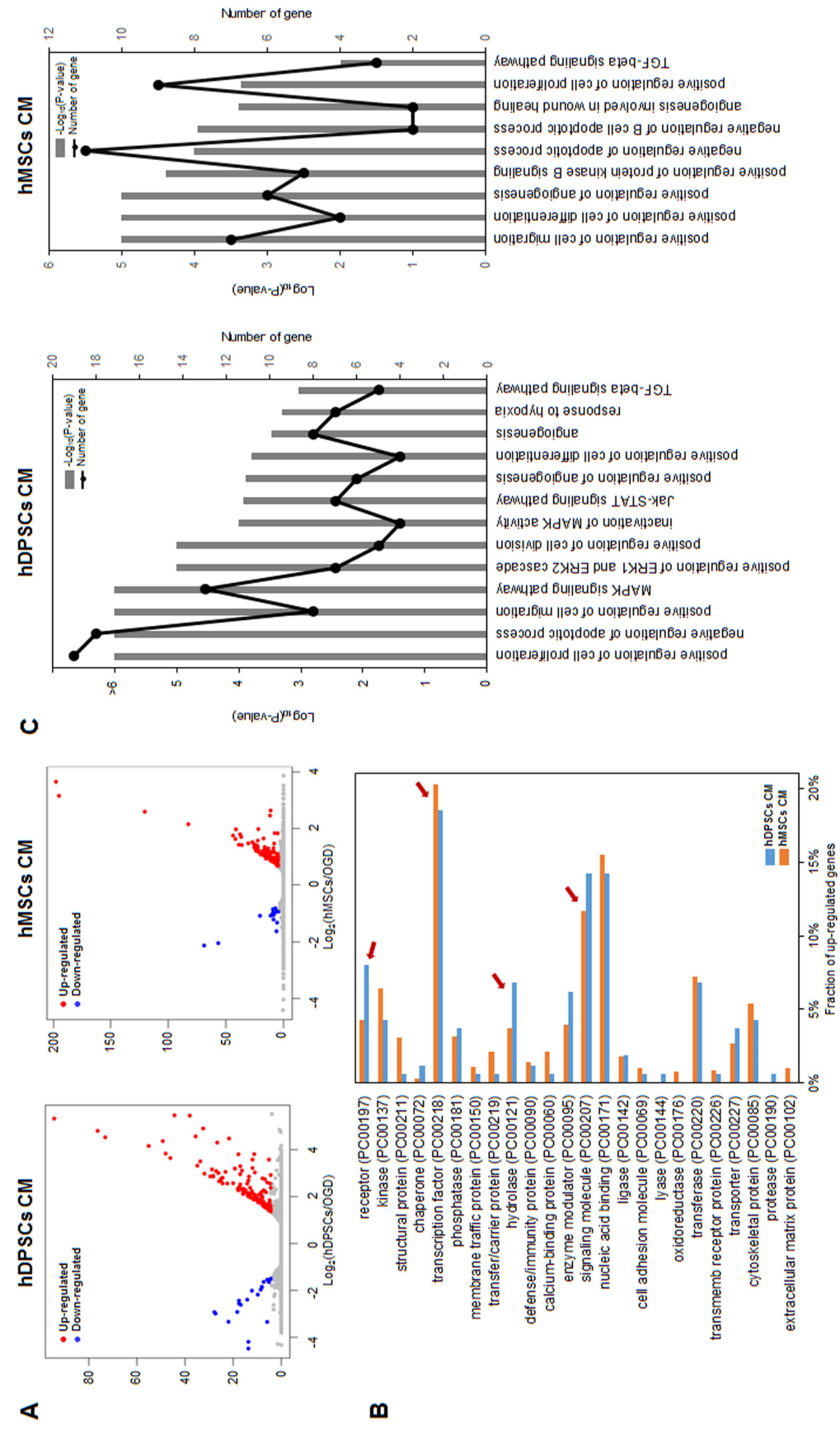

Figure 6. Gene expression profile differences in OGD-injured hAs treated with hDPSCs and hBM-MSCs. (A) Differential gene expression in OGD-injured control hAs and post-treatment of hDPSCs (left) or hBM-MSCs (right). Primary cultured hDPSCs and commercial hBM-MSCs were obtained from 10 and 3 donors separately. The *x*-axis represents the $\log_2$ fold changes, and the *y*-axis is the $-\log_{10}$-adjusted *p* value. Upregulated and downregulated genes in each treatment are colored red and blue, respectively. (B) Protein classification of genes upregulated in hDPSCs and hBM-MSCs. Four red arrows indicate the following protein classes: "receptor," "structural protein," "hydrolase," and "signaling molecule," showing the differences in the composition of upregulated genes between the treatments. (C) Gene ontology (GO) term and Kyoto Encyclopedia of Genes and Genomes (KEGG) pathway enrichment in genes upregulated in hDPSC- and hBM-MSC-treated hAs. The *p* values of significantly enriched terms or pathways and the number of the genes in the GO term and KEGG pathways are shown as bar plots ($-\log_{10} p$ value) and line graphs (number of genes in the specific enriched terms or pathways).

analysis package DESeq was used. A Venn diagram illustrating the overlap is shown in Figure 7A. In total, 66 common genes overlapped between 104 and 39 upregulated genes of the hDPSCs and hBM-MSCs, respectively (Fig. 7A). When we checked the enriched GO terms or KEGG pathways in the 66 common upregulated gene sets, there were common significant GO terms and KEGG pathways, such as the MAPK and TGF-β signaling pathways (Fig. 7B). Inactivation of MAPK activity and the MAPK signaling pathway were significantly induced in hDPSCs, versus hBM-MSCs (Fig. 7B).

As shown in Figure 7C, a qualitative clustering analysis and a comparison of the differential expression of selected MAPK and TGF-β pathway genes were performed, and heatmaps were generated. For the MAPK signaling pathway, growth arrest and DNA damage-inducible β (GADD45B), serum response factor (SRF), neurotrophin factor 4 (NTF4), and damage-suppressor protein 1 (DSUP1) genes were commonly upregulated in hDPSCs and hBM-MSCs. However, MAPK signaling pathways genes, including MAP kinase protein–serine kinase 3 (MAP2K3), fibroblast growth factor 5 (FGF5), platelet-derived growth factor subunit A (PDFGA), MYC, DUSP4, DUSP6, nuclear receptor subfamily 4 group A member 1 (NR4A1), fibroblast growth factor 18 (FGF18), and DUSP5, were markedly upregulated with hDPSCs versus with hBM-MSCs. For the TGF-β signaling pathway, inhibin β A (INHBA), thrombospondin 1 (THBS1), and Sma and mad-related family 7 (SMAD7) genes were commonly upregulated in hDPSCs and hBM-MSCs. Additionally, TGF-β pathway-related genes including MYC and growth differentiation factor 6 (GDF6) were upregulated with hDPSCs versus with hBM-MSCs (Fig. 7C).

DISCUSSION

This study demonstrated that the IV administration of hDPSCs after MCAo-induced cerebral stroke improved neurobehavioral function, similar to the improvement observed with hBM-MSC administration, and reduced greater infarct volume than treatment with hBM-MSCs at 28 days after MCAo. The mNSS test is a composite of motor, sensory, reflex, and balance tests[2,25]. It has been reported previously that hNSCs significantly promoted functional deficit recovery but did not significantly reduce the infarct area, compared with controls[26]. Thus, histological infarct volume did not directly indicate functional recovery. Our results are consistent with a previous report that porcine DPSC ($CD31^-/CD146^-$ side population cells) injection promoted motor disability recovery and reduced infarct volume after MCAo at 3 and 21 days in rats, compared with a PBS-injected group[8]. Similarly, transplantation of stem cells from human exfoliated deciduous teeth (SHED) into hypoxia–ischemia (HI)-injured mouse brain improved neurological function at 8 days after HI, compared with the PBS-treated group[27]. Moreover, intracerebral transplantation of hDPSCs 24 h following MCAo in a rat model improved forelimb sensorimotor function at 21 and 28 days after stroke[9]. Although we did not use primary cultured MSCs, commercial hBM-MSCs used in the present study are a suitable experimental model for studying differentiation in in vitro and in vivo ischemic stroke[2,3]. Differences between primary cultured hDPSCs and commercial hBM-MSCs in terms of proliferation, culture expansion, culture condition, and, especially, the culture medium may affect cerebral infarction volume and the functional outcome in a rat stroke model. Further investigation into the therapeutic mechanisms of primary cultured hBM-MSCs and commercial hBM-MSCs will help make this type of cell therapy a clinical option.

Our data indicated that IV-injected hDPSCs and hBM-MSCs survive, migrate along boundary zones adjacent to the lesion, and differentiate into neurons and astrocytes in the ischemic rat brain. These results are consistent with previous reports that grafted stem cells could differentiate into neurons and astrocytes in the microenvironment of the damaged brain in rat models of ischemia following IV injection[28,29]. Moreover, intracerebral engrafted hDPSCs migrated toward the stroke lesion and differentiated into astrocytes or neurons[9,27]. In the present study, a few of the originally IV-injected 4×10^6 HDPSCs were present in the brain at 4 weeks after ischemia. Chen et al. estimated that after IV administration of human umbilical cord blood (hUCB) in MCAo rats, only 1% of the injected cells were detected in the brain[30]. These results suggested that the majority of hDPSCs did not successfully cross the infarct-damaged blood–brain barrier (BBB). Direct cell-to-cell interactions between stem cells and local brain tissue might be a necessity for sufficient tissue restoration and neurogenesis, as suggested by studies wherein intracerebral transplantation of MSCs into the infarct area induced both neuroprotection and differentiation of endogenous stem cells[31]. However, the mechanisms of action of exogenous hDPSC treatment in various in vivo experiments have been attributed to the secretion of an array of factors resulting in paracrine effects. It has been shown that hDPSCs produce and secrete a broad variety of cytokines and growth factors such as nerve growth factor (NGF), brain-derived neurotrophic factor (BDNF), glial cell-derived neurotrophic factor (GDNF), and vascular endothelial growth factor (VEGF) that play important roles in the processes of neurogenesis and angiogenesis following brain injury and ischemia[32,33]. These autocrine and paracrine functions of hDPSCs can improve the microenvironment and make it more favorable for hosting cells.

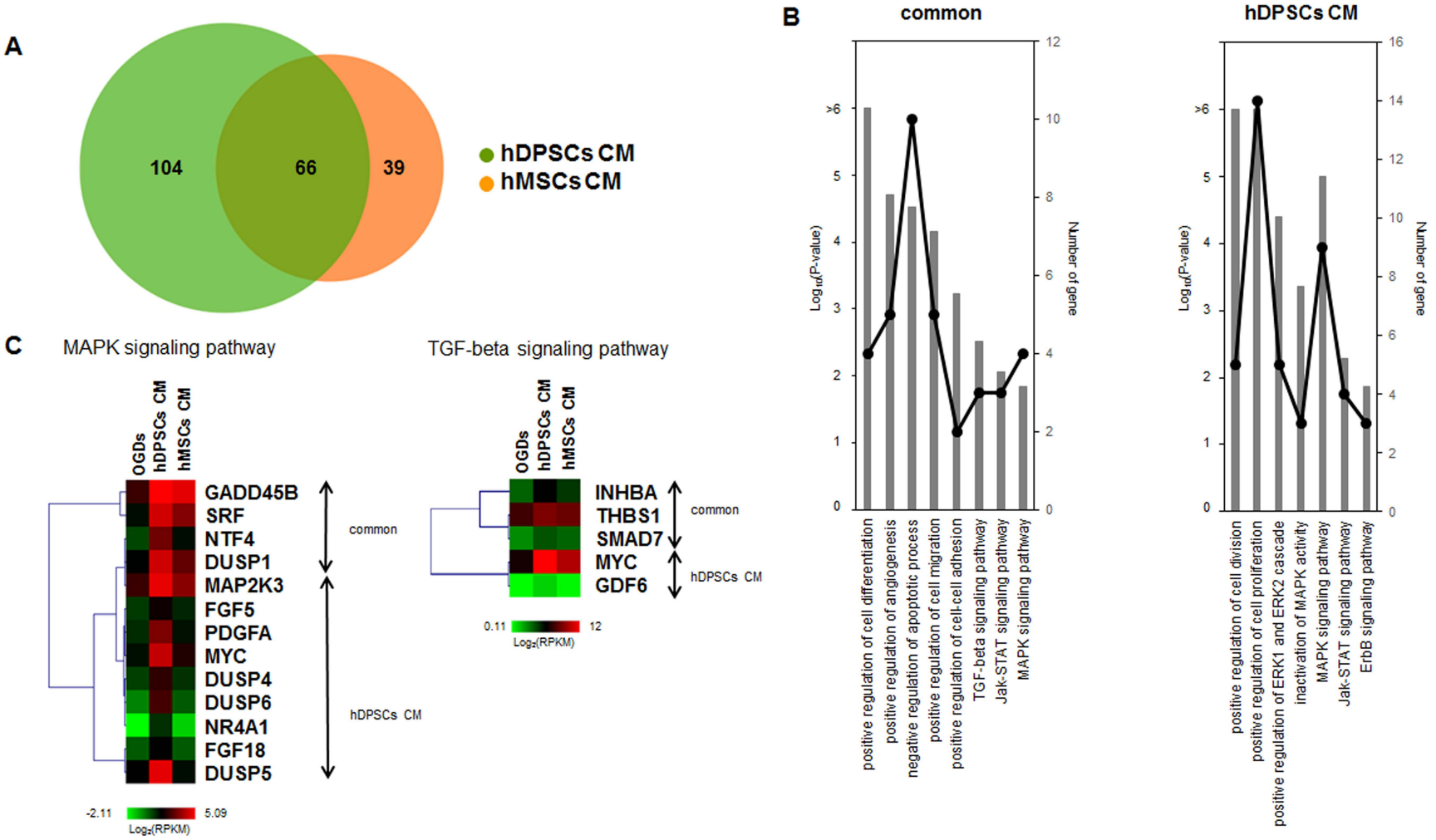

Figure 7. Comparison of hDPSC- and hBM-MSC-treated hA gene regulation. (A) Venn diagram of upregulated genes in hDPSC- and hBM-MSC-treated hAs. Primary cultured hDPSCs and commercial hBM-MSCs were obtained from 10 and 3 donors separately. (B) GO term and KEGG pathway enrichment of genes commonly (left) and exclusively (right) upregulated between the hDPSC- and hBM-MSC-treated groups. The overrepresented pathways and the numbers of genes in the GO terms and KEGG pathways are shown as bar plots ($-\log_{10} p$ value) and line graphs, similar to Figure 6C. (C) Heatmaps of the mitogen-activated protein kinase (MAPK) and transforming growth factor-β (TGF-β) signaling pathways. The expression values ($\log_2$ RPKM) of upregulated genes in hDPSCs and hBM-MSCs were calculated and used to perform hierarchal clustering and for generation of heatmaps. On the right side of the heatmap, the labels show the genes upregulated in both hDPSCs and hBM-MSCs and those upregulated exclusively in hDPSCs.

The precise mechanism of transplanted stem cells in experimental cerebral ischemia models remains unclear, but angiogenesis is thought to be an important contributing factor[25]. Transplanted MSCs can stimulate angiogenesis by secreting multiple angiogenic cytokines[34,35]. In the present study, an endothelial cell marker, vWF, showed a positive area in hDPSCs that was significantly larger than that with hBM-MSCs. Moreover, in our results, hDPSCs showed higher migratory ability in an in vitro Transwell culture system and higher in vitro angiogenic potential than hBM-MSCs. These in vivo and in vitro results are consistent with a previous report that subfractions of hDPSCs ($CD31^-/CD146^-$ SP cells and $CD105^+$ cells) demonstrated high angiogenic and neurogenic potential in mouse models of hindlimb ischemia[36]. Moreover, hDPSCs promoted endothelial migration significantly in in vitro Matrigel and migration assays and induced blood vessel formation in a chorioallantoic membrane assay[37]. These results indicate the higher in vivo and in vitro angiogenic potential of hDPSCs versus hBM-MSCs, which could potentially promote angiogenesis and neurogenesis in the injured brain after ischemic stroke.

In the present study, an acute host immune rejection, such as major infiltration of lymphocytes, directed toward the transplanted cells was not observed. Previous studies reported that hDPSCs display an increased level of immunosuppressive activities when compared with BM-MSCs. Huang et al. showed that the implantation of DPSCs derived from rhesus monkeys into the hippocampi of mice did not cause any immune rejection[38]. Similarly, higher expressions of human major histocompatibility complex 1 (MHC-1), which indicates a stronger degree of immunosuppression[40], were seen in mouse livers, which were incorporated with hDPSCs[39].

Central nervous system (CNS) insults, such as ischemia and neurodegenerative disease, induce reactive astrogliosis, characterized by increased expression of GFAP and hypertrophy[41,42]. GFAP and nestin upregulation are universally recognized as markers of reactive astrocytes[19]. In the present study, IV injection of hDPSCs decreased reactive gliosis significantly, as evidenced by the attenuation of cerebral ischemia-induced $GFAP^+$ and $nestin^+$ cells in rats, compared with the hBM-MSC-treated ischemic rats. These results are similar to a previous in vitro study with mouse bone marrow stromal cells[20]. Musashi-1 is considered a selective marker for neural stem/progenitor cells, similar to nestin. Moreover, $Musashi\text{-}1^+$ cells in the peri-infarct area after brain ischemia are regarded as reactive astrocytes, based on their coexpression of GFAP and nestin and their morphology[43]. In the present study, the $GFAP^+/Musashi\text{-}1^+$-stained area was suppressed significantly by hDPSCs and hBM-MSCs, suggesting that administration of hDPSCs and MSCs significantly inhibited astrogliosis.

Our in vivo findings were confirmed by in vitro data showing that treatment with hDPSCs had superior neuroprotective effects against OGD-induced cytotoxicity in hAs compared with hBM-MSCs. Our results are consistent with previous reports that hDPSCs release neuroprotective and anti-inflammatory molecules, resulting in the induction of neuronal rescue and survival[12,44]. These results suggest that administration of hDPSCs increased migration to ischemic hAs and enhanced angiogenesis, thus promoting neuroprotective effects in the ischemic brain.

Genome-wide gene expression profiling by RNA-Seq was used to investigate the molecular responses to hDPSCs and hBM-MSCs in the OGD-damaged hAs. In the present study, KEGG annotations showed that ERK1 and ERK2, JAK–STAT, MAPK, and TGF-β signaling pathways were abundant in hDPSCs. Most of these have already been reported as being involved in reactive astrogliosis[42]. For example, ERK[45], p38[46], and STAT3[47] signaling pathways were involved in glial scar formation and reactive astrocytes. Additionally, the TGF-β signaling pathway has been found to be essential for fibrous scar formation in the injured CNS[48,49].

p38 and ERK are activated by FGF, platelet-derived growth factor (PDGF), and NR4A1 in various cell types, including stem cells[50–52]. PDGF and FGF may be upregulated during acute brain lesions and induce progenitor cell migration in vitro and in vivo[44]. A DPSC graft elicited upregulated neurotrophic factors, such as VEGF, NGF, and FGF, in the hippocampi of immune-suppressed mice[54]. Furthermore, administration of FGF18 in the MCAo-induced stroke model in rats reduced infarct volumes and behavioral deficits[55]. FGF5, a neurotrophic growth factor, induced therapeutic angiogenesis[56]. NR4A1, also known as Nur77 and NGFIB, is a subfamily of nuclear receptors that function as transcription factors and is a novel protector for neural cells in an in vitro OGD model to mimic ischemic damage[57]. MAP2K3 phosphorylates and activates p38 during NSC differentiation[58]. V-Myc avian myelocytomatosis viral oncogene homolog (MYC) is one of the downstream genes of the MAPK pathways and plays an important role in the control of proliferation and survival of many cell types[59]. The specific dephosphorylation of MAPKs on both threonine and tyrosine residues is mediated by a subfamily of cysteine-dependent dual-specificity protein phosphatases (DUSPs), also known as MAPK phosphatases (MKPs)[60]. DUSP1, DUSP2, and DUSP4 display phosphatase activity toward both ERK1 and ERK2 and the stress-activated kinases, p38 and c-Jun N-terminal protein kinase (JNK)[61]. In contrast, DUSP5 is a growth factor-inducible gene and specifically interacts with and inactivates the ERK1/2 MAP kinases in mammalian cells[62]. DUSP6 is induced by FGF signaling and acts

as a negative regulator of ERK activity[63]. Our findings demonstrated that the expression of neurotropic factors such as FGF5, FGF18, and PDGFA, as well as MAPK upstream (MAP2K3 and DUSPs) or downstream pathway (MYC and NR4A1) genes, was significantly higher in the MAPK response genes of hDPSCs than that of hBM-MSCs. These results suggest that hDPSCs secreted growth factors as neurotrophic factors through the receptor protein kinase pathway, leading to phosphorylation of MAPK, and thus inducing activation of transcription factors, such as MYC and NR4A1.

The TGF-β pathway has been shown to be important in MSC differentiation into the neurogenic lineage[64]. Smad7 is an inhibitory Smad that is induced by TGF-β and represses TGF-β signaling by a negative feedback loop[65]. Myc and TGF-β signaling are mutually antagonistic; that is, Myc suppresses the activation of TGF-β-induced genes[66]. GDF6 (BMP13) is a member of the TGF-β superfamily, and its knockdown disrupts neural differentiation[67]. Our results indicate that the TGF-β signaling pathway was significantly enriched in the GO term and KEGG analyses. Additionally, the expression levels of GDF6 (TGF-β family of secreted signaling molecule) and MYC (feedback inhibitor for TGF-β) were significantly higher in the TGF-β response genes of hDPSCs than hBM-MSCs. These results suggest that hDPSCs activate TGF-β pathways within a negative feedback loop to limit the cell response. This observation further supports that Smad7 is an upregulated common gene in hDPSCs and hBM-MSCs.

CONCLUSION

In conclusion, this is the first reported study to demonstrate that IV transplantation of hDPSCs confers similar functional recovery and superior reduction of infarct size following MCAo in a rat model, compared with hBM-MSCs. The therapeutic benefit of hDPSCs may be due, in part, to high angiogenesis and neurogenic differentiation, and reduction of reactive gliosis in vivo, and hDPSCs protected damaged hAs targeting migration, and promoted angiogenic potential of hDPSCs in vitro through autocrine/paracrine mechanisms. GO term and KEGG pathway analyses provided molecular information regarding the mechanisms by which hDPSCs exert their effects in an in vitro stroke model. Thus, hDPSCs may provide a new and effective strategy for cell-based therapy in the treatment of ischemic diseases, such as stroke.

ACKNOWLEDGMENTS: This research was supported by the Basic Science Research Program through the National Research Foundation of Korea (NRF) funded by the Ministry of Education, Science and Technology (2015054225, NRF-2016R1A6A3A11931841, and 2012R1A5A2051384). The authors declare no conflicts of interest.

REFERENCES

1. Donnan GA, Fisher M, Macleod M, Davis SM. Stroke. Lancet 2008;10:1612–23.
2. Chen J, Li Y, Wang L, Zhang Z, Lu D, Lu M, Chopp M. Therapeutic benefit of intravenous administration of bone marrow stoma cells after cerebral ischemia in rats. Stroke 2001;32:1005–11.
3. Nomura T, Honmou O, Harada K, Houkin K, Hamada H, Kocsis JD. IV infusion of brain-derived neurotrophic factor gene-modified human mesenchymal stem cells protects against injury in a cerebral ischemia model in adult rat. Neuroscience 2005;136:161–9.
4. Lindvall O, Kokaia Z. Stem cell research in stroke: How far from the clinic? Stroke 2011;42:2369–75.
5. Gronthos S, Mankani M, Brahim J, Robey PG, Shi S. Postnatal human dental pulp stem cells (DPSCs) in vitro and in vivo. Proc Natl Acad Sci USA 2000;97:13625–30.
6. Inoue T, Sugiyama M, Hattori H, Wakita H, Wakabayashi T, Ueda M. Stem cells from human exfoliated deciduous tooth-derived conditioned medium enhance recovery of focal cerebral ischemia in rats. Tissue Eng Part A 2013;19: 24–9.
7. Pierdomenico L, Bonsi L, Calvitti M, Rondelli D, Arpinati M, Chirumbolo G, Becchetti E, Marchionni C, Alviano F, Fossati V, Staffolani N, Franchina M, Grossi A, Bagnara GP. Multipotent mesenchymal stem cells with immunosuppressive activity can be easily isolated from dental pulp. Transplantation 2005;27:836–42.
8. Sugiyama M, Iohara K, Wakita H, Hattori H, Ueda M, Matsushita K, Nakashima M. Dental pulp-derived $CD31^-$/$CD146^-$ side population stem/progenitor cells enhance recovery of focal cerebral ischemia in rats. Tissue Eng Part A 2011;17:1303–11.
9. Leong WK, Henshall TL, Arthur A, Kremer KL, Lewis MD, Helps SC, Field J, Hamilton-Bruce MA, Warming S, Manavis J, Vink R, Gronthos S, Koblar SA. Human adult dental pulp stem cells enhance poststroke functional recovery through non-neural replacement mechanisms. Stem Cells Transl Med. 2012;1:177–87.
10. Sakai K, Yamamoto A, Matsubara K, Nakamura S, Naruse M, Yamagata M, Sakamoto K, Tauchi R, Wakao N, Imagama S, Hibi H, Kadomatsu K, Ishiguro N, Ueda M. Human dental pulp-derived stem cells promote locomotor recovery after complete transection of the rat spinal cord by multiple neuro-regenerative mechanisms. J Clin Invest. 2012;122:80–90.
11. Stevens A, Zuliani T, Olejnik C, LeRoy H, Obriot H, Kerr-Conte J, Formstecher P, Bailliez Y, Polakowska RR. Human dental pulp stem cells differentiate into neural crest-derived melanocytes and have label-retaining and sphere-forming abilities. Stem Cells Dev. 2008;17:1175–84.
12. Yalvac ME, Rizvanov AA, Kilic E, Sahin F, Mukhamedyarov MA, Islamov RR, Palotás A. Potential role of dental stem cells in the cellular therapy of cerebral ischemia. Curr Pharm Des. 2009;15:3908–16.
13. Young F, Sloan A, Song B. Dental pulp stem cells and their potential roles in central nervous system regeneration and repair. J Neurosci Res. 2013;91:1383–93.
14. Iohara K, Zheng L, Wake H, Ito M, Nabekura J, Wakita H, Nakamura H, Into T, Matsushita K, Nakashima M. A novel stem cell source for vasculogenesis in ischemia: Subfraction of side population cells from dental pulp. Stem Cells 2008;26:2408–18.

15. Bakshi A, Hunter C, Swanger S, Lepore A, Fischer I. Minimally invasive delivery of stem cells for spinal cord injury: Advantages of the lumbar puncture technique. J Neurosurg Spine 2004;3:330–7.
16. Cho YA, Noh K, Jue SS, Lee SY, Kim EC. Melatonin promotes hepatic differentiation of human dental pulp stem cells: Clinical implications for the prevention of liver fibrosis. J Pineal Res. 2015;58:127–35.
17. Song M, Jue SS, Cho YA, Kim EC. Comparison of the effects of human dental pulp stem cells and human bone marrow-derived mesenchymal stem cells on ischemic human astrocytes in vitro. J Neurosci Res. 2015;93:973–83.
18. Song M, Kim Y, Kim Y, Ryu S, Song I, Kim SU, Yoon BW. MRI tracking of intravenously transplanted human neural stem cells in rat focal ischemia model. Neurosci Res. 2009;64:235–9.
19. Li L, Lundkvist A, Andersson D, Wilhelmsson U, Nagai N, Pardo AC, Nodin C, Ståhlberg A, Aprico K, Larsson K, Yabe T, Moons L, Fotheringham A, Davies I, Carmeliet P, Schwartz JP, Pekna M, Kubista M, Blomstrand F, Maragakis N, Nilsson M, Pekny M. Protective role of reactive astrocytes in brain ischemia. J Cereb Blood Flow Metab. 2008;28:468–81.
20. Gao Q, Li Y, Shen L, Zhang J, Zheng X, Qu R, Liu Z, Chopp M. Bone marrow stromal cells reduce ischemia-induced astrocytic activation in vitro. Neuroscience 2008; 152:648–55.
21. Wu TD, Nacu S. Fast and SNP-tolerant detection of complex variants and splicing in short reads. Bioinformatics 2010;26:873–81.
22. Anders S, Huber W. Differential expression analysis for sequence count data. Genome Biol. 2010;11:R106.
23. Thomas PD, Kejariwal A, Guo N, Mi H, Campbell MJ, Muruganujan A, Lazareva-Ulitsky B. Applications for protein sequence-function evolution data: mRNA/protein expression analysis and coding SNP scoring tools. Nucleic Acids Res. 2006;34:W645–50.
24. Lee JH, Gao C, Peng G, Greer C, Ren S, Wang Y, Xiao X. Analysis of transcriptome complexity through RNA sequencing in normal and failing murine hearts. Circ Res. 2011; 109:1332–41.
25. Onda T, Honmou O, Harada K, Houkin K, Hamada H, Kocsis JD. Therapeutic benefits by human mesenchymal stem cells (hMSCs) and Ang-1 gene-modified hMSCs after cerebral ischemia. J Cereb Blood Flow Metab. 2007;28: 329–40.
26. Song M, Kim YJ, Kim YH, Roh J, Kim SU, Yoon BW. Using a neodymium magnet to target delivery of ferumoxide-labeled human neural stem cells in a rat model of focal cerebral ischemia. Hum Gene Ther. 2010;21:603–10.
27. Yamagata M, Yamamoto A, Kako E, Matsubara K, Sakai K, Sawamoto K, Ueda M. Human dental pulp-derived stem cells protect against hypoxic-ischemic brain injury in neonatal mice. Stroke 2013;44:551–4.
28. Chu K, Kim M, Park KI, Jeong SW, Park HK, Jung KH, Lee ST, Kang L, Lee K, Park DK, Kim SU, Roh JK. Human neural stem cells improve sensorimotor deficits in the rat brain with experimental focal ischemia. Brain Res. 2004;1016:145–53.
29. Lee HJ, Kim KS, Kim EJ, Choi HB, Lee KH, Park IH, Ko Y, Jeong SW, Kim SU. Brain transplantation of immortalized human neural stem cells promotes functional recovery in mouse intracerebral hemorrhage stroke model. Stem Cells 2007;25:1204–12.
30. Chen J, Sanberg PR, Li Y, Wang L, Lu M, Willing AE, Sanchez-Ramos J, Chopp M. Intravenous administration of human umbilical cord blood reduces behavioral deficits after stroke in rats. Stroke 2001;32:2682–8.
31. Munoz JR, Stoutenger BR, Robinson AP, Spees JL, Prockop DJ. Human stem/progenitor cells from bone marrow promote neurogenesis of endogenous neural stem cells in the hippocampus of mice. Proc Natl Acad Sci USA 2005;102:18171–6.
32. Nosrat IV, Widenfalk J, Olson L, Nosrat CA. Dental pulp cells produce neurotrophic factors, interact with trigeminal neurons in vitro, and rescue motoneurons after spinal cord injury. Dev Biol. 2001;238:120–32.
33. Matsushita K, Motani R, Sakuta T, Yamaguchi N, Koga T, Matsuo K, Nagaoka S, Abeyama K, Maruyama I, Torii M. The role of vascular endothelial growth factor in human dental pulp cells: Induction of chemotaxis, proliferation, and differentiation and activation of the AP-1-dependent signaling pathway. J Dent Res. 2000;79:1596–603.
34. Zhang ZG, Zhang L, Jiang Q, Zhang R, Davies K, Powers C, Bruggen Nv, Chopp M. VEGF enhances angiogenesis and promotes blood-brain barrier leakage in the ischemic brain. J Clin Invest. 2000;106:829–38.
35. Zhang ZG, Zhang L, Jiang Q, Chopp M. Bone marrow-derived endothelial progenitor cells participate in cerebral neovascularization after focal cerebral ischemia in the adult mouse. Circ Res. 2002;90:284–8.
36. Nakashima M, Iohara K, Sugiyama M. Human dental pulp stem cells with highly angiogenic and neurogenic potential for possible use in pulp regeneration. Cytokine Growth Factor Rev. 2009;20:435–40.
37. Hilkens P, Fanton Y, Martens W, Gervois P, Struys T, Politis C, Lambrichts I, Bronckaers A. Pro-angiogenic impact of dental stem cells in vitro and in vivo. Stem Cell Res. 2014;12:778–90.
38. Huang AHC, Snyder BR, Cheng PH, Chan AW. Putative dental pulp-derived stem/stromal cells promote proliferation and differentiation of endogenous neural cells in the hippocampus of mice. Stem Cells 2008;26(10):2654–63.
39. Kim HJ, Cho YA, Lee YM, Lee SY, Bae WJ, Kim EC. PIN1 suppresses the hepatic differentiation of pulp stem cells via Wnt3a. J Dent Res. 2016;95(12):1415–24.
40. Hunt JS, Petroff MG, McIntire RH, Ober C. HLA-G and immune tolerance in pregnancy. FASEB J. 2005;19(7): 681–93.
41. Silver J, Miller JH. Regeneration beyond the glial scar. Nat Rev Neurosci. 2004;5:146–56.
42. Sofroniew MV. Molecular dissection of reactive astrogliosis and glial scar formation. Trends Neurosci. 2009;32:638–47.
43. Oki K, Kaneko N, Kanki H, Imai T, Suzuki N, Sawamoto K, Okano H. Musashi1 as a marker of reactive astrocytes after transient focal brain ischemia. Neurosci Res. 2010;66:390–5.
44. Norsat IV, Widenfalk J, Olsen L, Nosrat CA. Dental pulp cells produce neurotropic factors, interact with trigemimal neurons in vitro, and rescue motor neurons after spinal cord injury. Dev Biol. 2001;238:120–32.
45. Ito M, Natsume A, Takeuchi H, Shimato S, Ohno M, Wakabayashi T, Yoshida J. Type I interferon inhibits astrocytic gliosis and promotes functional recovery after spinal cord injury by deactivation of the MEK/ERK pathway. J Neurotrauma 2009;26:41–53.
46. Choudhury GR, Ryou M-G, Poteet E, Wen Y, He R, Sun F, Yuan F, Jin K, Yang SH. Involvement of p38 MAPK in

reactive astrogliosis induced by ischemic stroke. Brain Res. 2014;1551:45–58.
47. Herrmann JE, Imura T, Song B, Qi J, Ao Y, Nguyen TK, Korsak RA, Takeda K, Akira S, Sofroniew MV. STAT3 is a critical regulator of astrogliosis and scar formation after spinal cord injury. J Neurosci. 2008;28:7231–43.
48. Asher RA, Morgenstern DA, Fidler PS, Adcock KH, Oohira A, Braistead JE, Levine JM, Margolis RU, Rogers JH, Fawcett JW. Neurocan is upregulated in injured brain and in cytokine-treated astrocytes. J Neurosci. 2000;20:2427–38.
49. Diniz LP, Matias ICP, Garcia MN, Gomes FC. Astrocytic control of neural circuit formation: Highlights on TGF-beta signaling. Neurochem Int. 2014;78:18–27.
50. Baron W, Metz B, Bansal R, Hoekstra D, de Vries H. PDGF and FGF-2 signaling in oligodendrocyte progenitor cells: Regulation of proliferation and differentiation by multiple intracellular signaling pathways. Mol Cell Neurosci. 2000;15:314–29.
51. Ng F, Boucher S, Koh S, Sastry KS, Chase L, Lakshmipathy U, Choong C, Yang Z, Vemuri MC, Rao MS, Tanavde V. PDGF, TGF-beta, and FGF signaling is important for differentiation and growth of mesenchymal stem cells (MSCs): Transcriptional profiling can identify markers and signaling pathways important in differentiation of MSCs into adipogenic, chondrogenic, and osteogenic lineages. Blood 2008;112:295–307.
52. Zhou Y, Zhao W, Xie G, Huang M, Hu M, Jiang X, Zeng D, Liu J, Zhou H, Chen H, Wang GH, Zhang XK. Induction of Nur77-dependent apoptotic pathway by a coumarin derivative through activation of JNK and p38 MAPK. Carcinogenesis 2014;35:2660–9.
53. Lachapelle F, Avellana-Adalid V, Nait-Oumesmar B, Baron-Van Evercooren A. Fibroblast growth factor-2 (FGF-2) and platelet-derived growth factor AB (PDGF(AB)) promote adult SVZ-derived oligodendrogenesis in vivo. Mol Cell Neurosci. 2002;20:390–403.
54. Huang AH, Snyder BR, Cheng PH, Chan AW. Putative dental pulp-derived stem/stromal cells promote proliferation and differentiation of endogenous neural cells in the hippocampus of mice. Stem Cells 2008;26:2654–63.
55. Ellsworth JL, Garcia R, Yu J, Kindy MS. Fibroblast growth factor-18 reduced infarct volumes and behavioral deficits following occlusion of the middle cerebral artery in rats. Stroke 2003;34:1507–12.
56. Suzuki G, Lee TC, Fallavollita JA, Canty JM Jr. Adenoviral gene transfer of FGF-5 to hibernating myocardium improves function and stimulates myocytes to hypertrophy and reenter the cell cycle. Circ Res. 2005;96:767–75.
57. Xiao G, Sun T, Songming C, Cao Y. NR4A1 enhances neural survival following oxygen and glucose deprivation: An in vitro study. J Neurol Sci. 2013;330:78–84.
58. Skalnikova H, Vodicka P, Pelech S, Motlik J, Gadher SJ, Kovarova H. Protein signaling pathways in differentiation of neural stem cells. Proteomics 2008;8:4547–59.
59. Grandori C, Cowley SM, James LP, Eisenman RN. The Myc/Max/Mad network and the transcriptional control of cell behavior. Annu Rev Cell Dev Biol. 2000;16:653–99.
60. Camps M, Nichols A, Arkinstall S. Dual specificity phosphatases: A gene family for control of MAP kinase function. FASEB J. 2000;14:6–16.
61. Owens DM, Keyse SM. Differential regulation of MAP kinase signalling by dual-specificity protein phosphatases. Oncogene 2007;26:3203–13.
62. Mandl M, Slack DN, Keyse SM. Specific inactivation and nuclear anchoring of extracellular signal-regulated kinase 2 by the inducible dual-specificity protein phosphatase DUSP5. Mol Cell Biol. 2005;25:1830–45.
63. Ekerot M, Stavridis MP, Delavaine L, Mitchell MP, Staples C, Owens DM, Keenan ID, Dickinson RJ, Storey KG, Keyse SM. Negative-feedback regulation of FGF signalling by DUSP6/MKP-3 is driven by ERK1/2 and mediated by Ets factor binding to a conserved site within the DUSP6/MKP-3 gene promoter. Biochem J. 2008;412:287–98.
64. He Y, Zhang H, Yung A, Villeda SA, Jaeger PA, Olayiwola O, Fainberg N, Wyss-Coray T. ALK5-dependent TGF-β signaling is a major determinant of late-stage adult neurogenesis. Nat Neurosci. 2014;17:943–52.
65. Yan X, Liu Z, Chen Y. Regulation of TGF-beta signaling by Smad7. Acta Biochim Biophys Sin. (Shanghai) 2009;41:263–72.
66. Itoh S, Itoh F. Inhibitory machinery for the TGF-β family signaling pathway. Growth Factors 2011;29:163–73.
67. Hanel ML, Hensey C. Eye and neural defects associated with loss of GDF6. BMC Dev Biol. 2006;6:43.
68. Benjamini Y, Hochberg Y. Controlling the false discovery rate: A practical and powerful approach to multiple testing. J Roy Stat Soc B 1995;57:289–300.